Available online at www.sciencedirect.com
ScienceDirect
Surface Science 602 (2008) 1428–1432
SURFACE SCIENCE
www.elsevier.com/locate/susc

Desorption of hydrogen from InN(000$\bar{1}$) observed by HREELS

R.P. Bhatta, B.D. Thoms *, M. Alevli, N. Dietz

Department of Physics and Astronomy, Georgia State University, Atlanta, GA 30303, United States

Received 14 October 2007; accepted for publication 5 February 2008
Available online 12 February 2008

Abstract

The kinetics of isothermal desorption of hydrogen from InN(000$\bar{1}$) have been investigated using surface vibrational spectroscopy. Reductions in intensity of the N–H stretching and bending vibrations in high resolution electron energy loss spectra (HREELS) upon annealing indicated loss of surface hydrogen and was attributed to recombinative desorption. Hydrogen completely desorbs from the InN surface upon annealing for 900 s at 425 °C or upon annealing for 30 s at 500 °C. Surface hydrogen coverage was determined using the intensity of the N–H stretching vibrational loss peak. Fitting the coverage versus temperature for anneals of either 30 or 900 s indicated that the desorption was best described by second-order desorption kinetics with an activation energy and pre-exponential factor of 1.3 ± 0.2 eV and $10^{-7.3\pm1.0}$ cm^2/s, respectively. In addition to thermal desorption, an increase in the carrier concentration in the film was also observed upon annealing to 450 °C or higher as shown in HREELS by a shift of the conduction band plasmon excitation to higher energy.

Keywords: Electron energy loss spectroscopy; Indium nitride; Hydrogen; Desorption

1. Introduction

Group III-nitride semiconductors GaN, AlN, InN and their alloys are promising materials for photonic, optoelectronic and microelectronic devices [1–3]. InN, one of the least studied nitride semiconductors, is a potential material for a wide range of applications including high electron mobility transistors [4], chemical and biological sensors [5], transparent conducting window material for heterojunction solar cells [6], thermoelectric devices [7] and terahertz radiation devices [8]. The development of the indium-rich InGaN alloy system will allow for tuning of the band gap over a wide spectral range from blue to infrared [9].

Surface reactions involving hydrogen are important steps in the growth mechanism of InN thin films. Surface hydrogen atoms produced by the decomposition of precursors during InN growth are most frequently eliminated by desorption after reacting with adsorbed methyl groups or other hydrogen atoms. Adsorbed hydrogen reduces the number of available reaction sites for indium and nitrogen precursors. Koukitu et al. [10] carried out a detailed thermodynamic study on the role of hydrogen during metal–organic chemical vapor deposition (MOCVD) growth of Group III-nitrides and showed that an increase in hydrogen partial pressure due to decomposition of growth precursors results in a decrease of the InN deposition rate and that the increase in H_2 can drive the system from the deposition mode into the etching mode. Hydrogen in the growth environment also affects the film composition. Losurdo et al. [11] reported that InN strongly reacts with atomic hydrogen causing depletion of nitrogen and the concurrent formation of indium droplets at the surface. Scholz et al. [12] reported that the indium incorporation rate in the growth of InGaN was nearly doubled when reducing the hydrogen content in the growth chamber. Piner et al. [13] reported that the indium content drops significantly as the hydrogen flow increases for MOCVD-grown InN layers and atomic-layer-deposited InGaN.

Understanding the various effects of hydrogen on growth under a range of process conditions requires knowledge of

* Corresponding author. Tel.: +1 404 4136045; fax: +1 404 4136025.

0039-6028/$ - see front matter © 2008 Elsevier B.V. All rights reserved.
doi:10.1016/j.susc.2008.02.003

the kinetic parameters for surface reactions. However, both qualitative and quantitative details of many of the important surface reactions occurring during InN growth are not yet known. In this work, high resolution electron energy loss spectroscopy (HREELS) has been used to determine the kinetic parameters for hydrogen desorption from the N-polar InN surface. In addition, the effects of heating on surface structure and electronic properties are also reported.

2. Experimental methods

Two InN samples, referred to as samples A and B, grown by high pressure chemical vapor deposition (HPCVD) under similar conditions were investigated. The layers were grown at a temperature of ~810 °C, reactor pressure of 15 bar, and ammonia to trimethylindium ratios of 790 (sample A) and 630 (sample B). The layers were deposited on a GaN buffer layer grown on a sapphire (0001) substrate. Details of the HPCVD reactor, growth configuration, and real-time optical characterization techniques employed have been published elsewhere [14,15]. The samples were transported in air before being introduced into the ultrahigh vacuum chamber (UHV) surface characterization system. The UHV chamber had a base pressure of 1.8×10^{-10} torr and details of the surface science apparatus have been published previously [16]. Before introduction into the UHV chamber, the InN sample was rinsed with isopropyl alcohol, mounted on a tantalum sample holder, and held in place by tantalum clips. Sample heating was achieved by electron bombardment of the back of the tantalum sample holder. A chromel–alumel thermocouple was attached to the mount next to the sample to record the sample temperature.

Auger electron spectroscopy (AES) of the as-inserted InN samples revealed oxygen and carbon contamination due to the exposure of sample to the atmosphere. Sample cleaning was achieved in two steps. In the first step, most of the carbon contaminants were removed by 0.5 keV argon ion sputtering at a glancing angle of 70° from the surface normal. In second step, atomic hydrogen cleaning (AHC) was performed by backfilling the vacuum chamber with hydrogen to a pressure of 8.4×10^{-7} torr in the presence of a tungsten filament heated to 1575 °C to produce atomic hydrogen. The sample was positioned 20 mm from the filament for 20 min (giving an exposure of 1000 L of H_2). The sample temperature rose to approximately 75 °C, due to the proximity of the heated filament. After this, the sample was heated to 325 °C while remaining in front of the tungsten filament for an additional 20 min (an additional 1000 L of H_2).

The AES spectra after cleaning confirmed that the InN surface is free from contaminants. Low energy electron diffraction (LEED) showed a hexagonal 1×1 LEED pattern, demonstrating a well ordered surface. After cleaning, sample A was annealed to a series of temperatures from 375 to 425 °C for 900 s and the sample B was annealed at temperatures from 425 to 500 °C for 30 s. The surface was restored to its original condition through AHC between annealing treatments. HREELS experiments were performed in a specular geometry with incident and scattering angles of 60° from the normal and incident electron energy of 7.0 eV. The instrumental resolution determined from full width at half maximum of the elastic peak was 60 cm^{-1}.

3. Results and discussion

HREEL spectra from sample A, taken after AHC and annealing to various temperatures for 900 s, are shown in Fig. 1. In the spectrum taken after AHC, a prominent peak appears at a loss energy of 560 cm^{-1} and is assigned to the Fuchs–Kliewer surface phonon [17]. The peaks at 3260 and 860 cm^{-1} are assigned to N–H stretching and bending vibrational modes, respectively [18]. At high hydrogen coverages, a small peak was observed at 1430 cm^{-1} and is assigned to a combination loss of the Fuchs–Kliewer phonon and the N–H bending vibration. The presence of N–H vibrations and the lack of In–H features indicates that the layer is nitrogen terminated consistent with N-polar InN(000$\bar{1}$) [19,20]. A broad feature centered at a loss energy of ~3800 cm^{-1} is due to the conduction band plasmon excitation [19,20].

The loss features in Fig. 1 due to Fuchs–Kliewer surface phonons and the conduction band plasmon excitation do not change upon annealing. After annealing to 375 °C, the intensity of both N–H stretch and bend decrease and disappear completely after heating the sample to 425 °C for 900 s. The reductions in intensity of N–H vibrations are attributed to recombinative desorption of hydrogen. In addition to the N–H vibrational peaks, a small feature

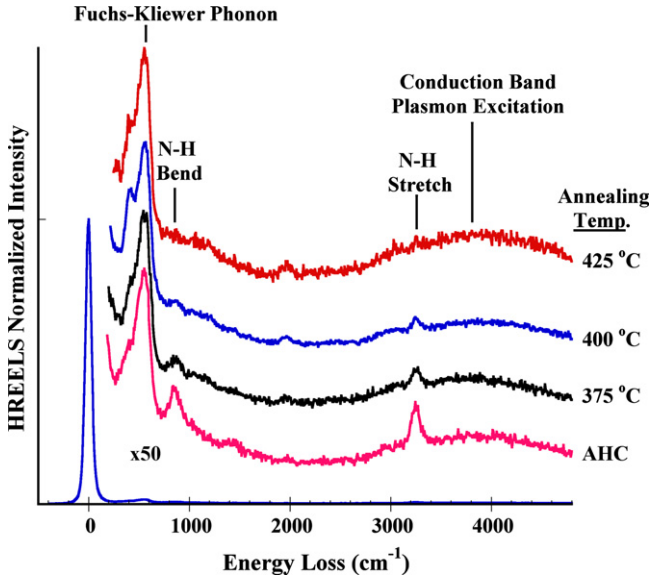

Fig. 1. HREEL spectra from sample A after preparation by atomic hydrogen cleaning (AHC) and after heating for 900 s to 375, 400, and 425 °C. The surface was restored to the same initial state with AHC prior to each heat treatment.

appears at 2000 cm^{-1} as the N–H vibrations decrease. Although no firm assignment is made, the authors suggest that it may be due to a surface N–N vibrational mode. N–N stretching vibrational modes have been reported to occur over a wide range of frequencies. de Paola et al. [21] and Anton et al. [22] reported (N–N) on Ru (001) at 2195 cm^{-1} and 2200–2250 cm^{-1}, respectively. Grunze et al. [23] observed the N–N stretching mode on a Ni surface to be at 1490 cm^{-1} while Apen and Gland [24] identified the N–N stretching mode on the GaAs surface is at 1671 cm^{-1}. The wide range of frequencies observed for N–N stretches makes a firm assignment here difficult, but does demonstrate that it is possible for the 2000 cm^{-1} peak to be due to a surface N–N bond.

Fig. 2 shows the results of a similar experiment on sample B, although with anneal times of 30 s. The spectrum acquired after AHC shows the same N–H vibrations at 860, 1430, and 3260 cm^{-1} as well as the Fuchs–Kliewer phonon at 560 cm^{-1} as observed on sample A. However, a small C–H stretching vibrational peak is observed at 2950 cm^{-1} due to a small amount of residual carbon contamination on sample B. Also, the conduction band plasmon excitation is observed at a slightly lower frequency than on sample A indicating a slightly lower plasma frequency and therefore slightly lower carrier concentration. Samples A and B were grown using different ammonia to TMI ratios of 790 and 630, respectively, and are unintentionally n-type doped. The small difference in bulk carrier concentration would not be expected to significantly affect the process of hydrogen recombinative desorption.

As shown in Fig. 2, partial desorption of hydrogen is observed for anneals from 425 to 475 °C as seen by reductions in the N–H vibrations, while complete desorption of hydrogen is observed after heating to 500 °C for 30 s.

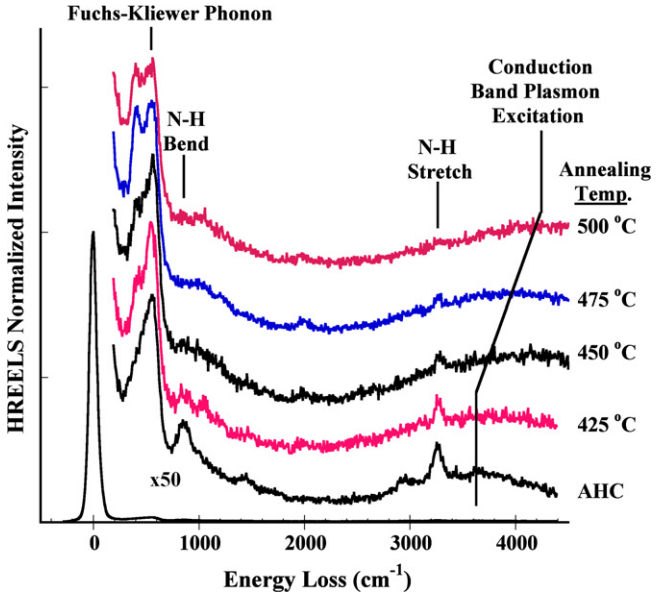

Fig. 2. HREEL spectra from sample B after preparation by atomic hydrogen cleaning (AHC) and after heating for 30 s to 425, 450, 475, and 500 °C. The surface was restored to the same initial state with AHC prior to each heat treatment. The line marking the conduction band plasmon excitation is only provided as a guide to the eye.

There have been no published studies of hydrogen desorption from InN, but several groups have reported results for hydrogen desorption from N-polar GaN. Sung et al. [25] reported the desorption of hydrogen from the nitrogen sites on a GaN surface at 850 °C. In contrast, Chiang et al. [26] reported hydrogen desorption from Ga-sites of a GaN surface at 250 °C and from the N-sites at 500 °C. The desorption temperature from N-sites on InN reported in this paper is similar to the result for N-sites on GaN reported by Chiang et al. but much lower than that reported by Sung et al.

Understanding the mechanisms and kinetics of hydrogen desorption is important for developing both qualitative and quantitative models of the growth of indium-rich III-nitrides. The main source of hydrogen in MOCVD may come from carrier gas and the decomposition of ammonia precursors [27]. The methyl groups and hydrogen atoms formed during decomposition combine and may form methane (CH_4), ethane (C_2H_6) or molecular hydrogen (H_2), which desorb from the growth surface. The temperature region suitable for the deposition of high quality InN by MOCVD has been reported from 500 to 650 °C, while it ranges from 450 to 550 °C in molecular beam epitaxy [9] and from 455 to 510 °C for halide vapor phase epitaxy [28]. This growth temperature regime suggests that the typical growth temperature of InN is in the same order at which hydrogen desorbs (425–500 °C) from the InN surface. If the growth temperature would be lower than the hydrogen desorption temperature, sites on the InN growth surface could be occupied by hydrogen, which is produced during the precursor decomposition process. This would reduce the number of reaction sites available for adsorption of indium or nitrogen precursors and could affect the growth rate. At temperatures higher than required for hydrogen recombination, hydrogen desorption increases the number of reaction sites for precursors and may enhance the growth rate. At much higher surface temperatures, additional InN dissociation and the desorption of molecular nitrogen may occur [29,30].

The process of annealing at higher temperature also affects the electronic properties of the film. The broad loss feature due to the conduction band plasmon excitation peaked at ~3700 cm^{-1} for sample B after AHC and remained unchanged after annealing to 425 °C. However, annealing to 450 °C or above produced a shift of the plasmon excitation peak to higher energy, with the plasmon loss peaking at ~4200 cm^{-1} after heating to 500 °C for 30 s. The increase in plasmon loss energy indicates a higher plasma frequency, correlating to an increase in the carrier concentration. This is consistent with the report of Huang et al. [31] who pointed out that the carrier concentration rapidly increases while carrier mobility rapidly decreases from the as grown values for InN grown by MBE, when annealed above 550–600 °C.

As shown in Fig. 2, the annealing of the sample at 475 °C or above result in a new HREELS peak at

400 cm^{-1}. The small vibrational frequency of this peak may indicate that it involves the bonding between surface nitrogen and the second layer indium atoms. After annealing for 30 s at 475 °C, several cycles of AHC are required to remove this new feature and to regain the initial surface ordering. Desorption kinetic parameters are often determined by performing temperature programmed desorption (TPD) experiments, however, in the case of hydrogen desorption from InN it would require temperatures in excess of 500 °C. Since heating to those temperatures may cause changes in the In–N bonds in the surface region as indicated by the development of the 400 cm^{-1} loss peak, HREEL spectra were used to determine kinetic parameters instead of TPD data.

To determine kinetic parameters from HREELS data, relative surface coverages were obtained by integrating the area under the N–H stretching vibrational peak in each normalized HREEL spectrum. A smooth background was assumed for the underlying conduction band plasmon loss. The normalized N–H stretch intensity is expected to be proportional to the surface coverage [32] since it has been shown in earlier work by the authors to be due to dipole scattering [19]. Plots of normalized N–H intensity versus annealing temperature are shown in Fig. 3 and Fig. 4 for 900 and 30 s annealing times, respectively. Although the sample was annealed to 325 °C during AHC, the exposure with atomic hydrogen continued until the sample cooled down to ~200 °C. Therefore, N–H stretch intensities from each sample after AHC are plotted as equivalent to a 200 °C anneal.

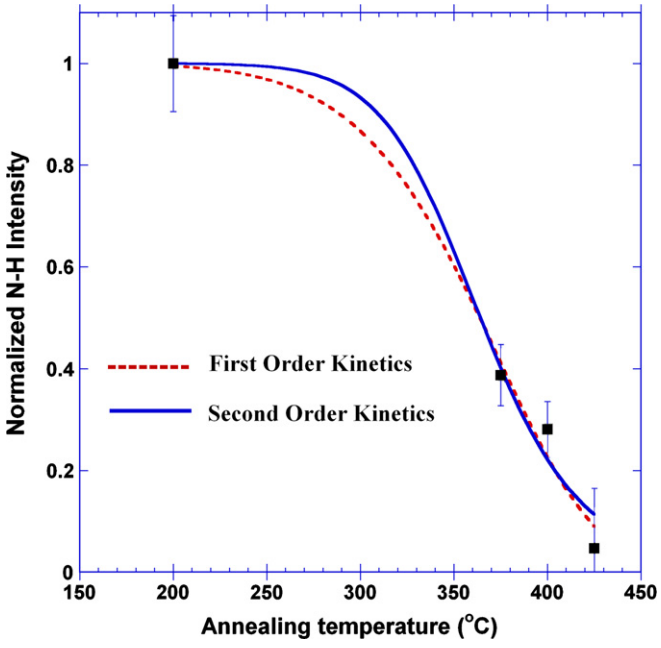

Fig. 3. Fitting of first and second-order desorption kinetics to hydrogen coverage (determined from HREELS N–H stretch intensity) for InN sample A after preparation by atomic hydrogen cleaning and after heating for 900 s to 375, 400, and 425 °C. Equation and parameters used in the fitting are described in the text.

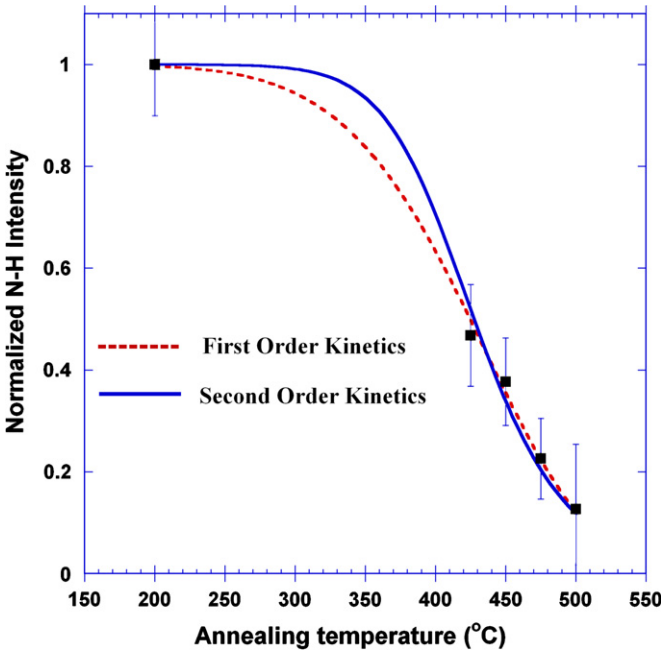

Fig. 4. Fitting of first and second-order desorption kinetics to hydrogen coverage (determined from HREELS N–H stretch intensity) for InN sample B after preparation by atomic hydrogen cleaning and after heating for 30 s to 425, 450, 475, and 500 °C. Equation and parameters used in the fitting are described in the text.

The data were fitted using both first-order and second-order desorption kinetics. For first-order desorption the integrated intensities were fit using

$$\frac{\theta}{\theta_0} = e^{-\nu_1 t \exp(-E/kT)}$$

where θ is the surface hydrogen coverage, θ_0 is the initial coverage, t is the anneal time, ν_1 is the first-order pre-exponential factor, and E is the activation energy. From the fitting for first-order desorption kinetics, no common set of values for activation energy and pre-exponential factor were found which produced good fits to both the 900 and 30 s anneal time data. The best individual first-order fits were found to have an activation energy and pre-exponential factor, respectively, of 0.8 eV and 1100 s^{-1} for 900 s anneals and 0.7 eV and 2100 s^{-1} for 30 s anneals. The pre-exponential factors determined in these fits are far below the values expected. For the desorption of atoms that are mobile on the surface, a first-order or pseudo first-order pre-exponential factor in the range of 10^{13} s^{-1} is expected. For atoms that are immobile on the surface, the factor would be in the range of 10^{16}–10^{17} s^{-1} [33]. For second-order desorption, the integrated intensities were fit using

$$\frac{\theta}{\theta_0} = \frac{1}{1 + \theta_0 \nu_2 t e^{-E/kT}}$$

where θ is the surface hydrogen coverage, θ_0 is the initial coverage, t is the anneal time, ν_2 is the second-order pre-exponential factor, and E is the activation energy. Fitting to second-order desorption kinetics yields a good fit to

both sets of data using a common set of kinetic parameters with an activation energy of 1.3 ± 0.2 eV and a second-order pre-exponential factor of $10^{-7.3\pm1.0}$ cm^2/s (equivalent to a pseudo-first-order pre-exponential factor of $10^{7.5\pm1.0}$ s^{-1}). Therefore, we conclude that these data are more consistent with second-order desorption kinetics, which is typical of hydrogen recombination on most III–V semiconductor surfaces.

The number of temperatures used in each desorption series limits the accuracy of the activation energy determined here. Even so, an activation energy of 1.3 eV for recombinative desorption of hydrogen indicates considerable energy is reclaimed by surface relaxation or re-bonding of the surface nitrogen atoms. This re-bonding is consistent with the development of a HREELS loss peak at 2000 cm^{-1} upon hydrogen desorption as seen in Figs. 1 and 2 and supports the suggestion that this peak is due to N–N bonding.

4. Summary and conclusions

The desorption of hydrogen from InN$(000\bar{1})$ was investigated by high resolution electron energy loss spectroscopy. Complete removal of surface hydrogen was observed after heating to 425 °C for 900 s or 500 °C for 30 s. The desorption is best described by second-order kinetics with an activation energy of 1.3 ± 0.2 eV and a pre-exponential factor of $10^{-7.3\pm1.0}$ cm^2/s. Annealing to 450 °C or above produces a shift in conduction band plasmon excitation peak to higher loss energy demonstrating an increase in the free carrier concentration in the film.

Acknowledgements

The authors would like to acknowledge support of this work by AFOSR Grant FA9550-07-1-0345 and GSU-RPE. Authors would also like to thank Ananta Acharya for assistance in data analysis and manuscript preparation.

References

[1] O. Ambacher, J. Phys. D: Appl. Phys. 31 (1998) 2653.
[2] S.N. Mohammad, H. Morkoc, Prog. Quant. Electr. 20 (1996) 361.
[3] S. Strife, H. Morkoc, J. Vac. Sci. Technol. B 10 (1992) 1237.
[4] M. Singh, J. Singh, J. Appl. Phys. 94 (2003) 2498.
[5] H. Lu, W.J. Schaff, L.F. Eastman, J. Appl. Phys. 96 (2004) 3577.
[6] A. Yamamoto, M. Tsujino, M. Ohkubo, A. Hashimoto, Sol. Energy Mater. 35 (1994) 53.
[7] S. Yamaguchi, R. Izaki, N. Kaiwa, S. Sugimura, A. Yamamoto, Appl. Phys. Lett. 84 (2004) 5344.
[8] Y.M. Meziani, B. Maleyre, M.L. Sadowski, S. Ruffenach, O. Briot, W. Knap, Phys. Status Solidi (a) 202 (2005) 590.
[9] A.G. Bhuiyan, A. Hashimoto, A. Yamamoto, J. Appl. Phys. 94 (2003) 2779.
[10] A. Koukitu, T. Taki, N. Takahashi, H. Seki, J. Cryst. Growth 197 (1999) 99.
[11] M. Losurdo, M.M. Giangregori, G. Bruno, T.H. Kim, P. Wu, S. Choi, M. Morse, A. Brown, F. Masia, A. Polimeni, M. Capizzi, Mater. Res. Symp. Proc. 892 (2006) FF08.
[12] F. Scholz, V. Harle, F. Steuber, H. Bolay, A. Dornen, B. Kaufmann, V. Syganow, A. Hangleiter, J. Cryst. Growth 170 (1997) 321.
[13] E.L. Piner, M.K. Behbehani, N.A. ElMasry, F.G. McIntosh, J.C. Roberts, K.S. Boutros, S.M. Bedair, Appl. Phys. Lett. 70 (1997) 461.
[14] V. Woods, J. Senawirante, N. Dietz, J. Vac. Sci. Technol. B 23 (2005) 1790.
[15] N. Dietz, M. Strassburg, V. Woods, J. Vac. Sci. Technol. A 23 (2005) 1221.
[16] V.J. Bellitto, B.D. Thoms, D.D. Koleske, A.E. Wickenden, R.L. Henry, Surf. Sci. 430 (1999) 80.
[17] R. Fuchs, K.L. Kliewer, Phys. Rev. 140 (1965) A2076.
[18] R.P. Bhatta, B.D. Thoms, M. Alevli, V. Woods, N. Dietz, Appl. Phys. Lett. 88 (2006) 122112.
[19] R.P. Bhatta, B.D. Thoms, M. Alevli, N. Dietz, Surf. Sci. 601 (2007) L120.
[20] R.P. Bhatta, B.D. Thoms, A. Weerasekara, A.G.U. Perera, M. Alevli, N. Dietz, J. Vac. Sci. Technol. A 25 (2007) 967.
[21] R.A. de Paola, F.M. Hoffmann, D. Heskett, E.W. Plummer, Phys. Rev. B 35 (1986) 4236.
[22] A.B. Anton, N.R. Avery, B.H. Toby, W.H. Weinberg, J. Electron Spectrosc. Relat. Phenom. 29 (1983) 181.
[23] M. Grunze, M. Golze, W. Hirschwald, H.-J. Freund, H. Pulm, U. Seip, M.C. Tsai, G. Etrl, J. Kuppers, Phys. Rev. Lett. 53 (1984) 850.
[24] E. Apen, J.L. Gland, Surf. Sci. 321 (1994) 308.
[25] M.M. Sung, J. Ahn, V. Bykov, J.W. Rabalais, D.D. Koleske, A.E. Wickenden, Phys. Rev. B 54 (1996) 14652.
[26] C.M. Chiang, S.M. Gates, A. Bensaoula, J.A. Schultz, Chem. Phys. Lett. 246 (1995) 275.
[27] B.H. Cardelino, C.E. Moore, S.D. McCall, C.A. Cardelino, N. Dietz, K. Bachmann, CAITA-2004, ISBN 86-7466-117-3, 2004, 1.
[28] Y. Sato, S. Sato, J. Cryst. Growth 144 (1994) 15.
[29] A.G. Bhuiyan, A. Yamamoto, A. Hashimoto, Y. Ito, J. Cryst. Growth 236 (2002) 59.
[30] Q. Guo, O. Kato, A. Yoshida, J. Appl. Phys. 73 (1993) 7969.
[31] W. Huang, M. Yoshimoto, K. Taguchi, H. Harima, J. Saraie, Jpn. J. Appl. Phys. 43 (2004) L97.
[32] H. Ibach, D.L. Mills, Electron Energy Loss Spectroscopy and Surface Vibrations, Academic Press, New York, 1982.
[33] G.A. Somorjai, Chemistry in Two Dimensions: Surfaces, Cornell University Press, 1981.